Effect of Prestrain on Ductility of a X100 Pipeline Steel

Jacques Besson[1, a], Yasuhiro Shinohara,[1, b], Thilo F. Morgeneyer[1, c], Yazid Madi[1, 2, d]

[1] Centre des Matériaux, Mines Paris, Paristech, CNRS UMR 7633
BP 87, 91003 Evry Cedex, France
[2] Ermess, EPF - Ecole d'Ingénieurs, 3 bis, rue Lakanal 92330 Sceaux, France
[a] jacques.besson@ensmp.fr, [b] yasuhiro.shinohara@mat.ensmp.fr, [c] thilo.morgeneyer@ensmp.fr,
[d] yazid.madi@mat.ensmp.fr

Keywords: Prestrain, X100 steel, ductile rupture, anisotropy, toughness

Abstract. The plastic behavior of a X100 steel plate is studied showing plastic anisotropy and combinaison of isotropic and kinematic hardening. Ductility and toughness of the material is tested along different loading directions using notched tensile bars and C(T) specimens. It is shown that the rolling direction (L) presents better properties than the long transverse direction (T). Prestraining the material by 6% along the T direction reduces the ductility of tensile bars by 3 to 7% but strongly reduced toughness (measured on C(T) specimens according to the ASTM-1820 standard): 28% for the L-T configuration and 40% for the T-L configuration.

Introduction

Metal sheets are often prestrained during the last stages of processing and during forming operations. This is the case of aluminium sheets used to manufacture aircraft fuselage or of steel plates used to produce pipeline elements with the pipe forming processes such as UOE, electric resistance welding (ERW), Roll bending. Moreover, line pipes are subjected to plastic bending due to ground movements in operation. Prestrain both hardens and damages materials so that fracture properties (e.g. ductility and toughness) of the final product may differ from those of the unstrained material. As hardening is often both isotropic and kinematic prestrain can induce anisotropic hardening properties in addition to the texture related plastic anisotropy [1].

Material mechanical testing

Material. The material of this study is an experimental X100 grade high strength steel. This class of steel is used to manufacture pipelines. It was supplied as a 16 mm thick plate. The nominal chemical composition is given on Table 1. The plate was elaborated using thermo-mechanical controlled rolling and accelerated cooling (TMCP process). The resulting microstructure is mainly a dual phase structure consisting of fine polygonal ferrite and bainite (Fig. 1).

Due to material processing, the plate has an anisotropic plastic behaviour [2] so that it is important to keep track of the material principal axes. In the following the longitudinal direction corresponding to the rolling direction is referred to as L; the transverse direction is referred to as T and the short transverse (thickness) direction is referred to as S. D stands for the diagonal direction (45 between direction L and T in the sheet plane).

In order to prestrain the material, large flat tensile specimens (see Fig. 2) were machined and strained up to 6% on a 4000 kN tensile machine. The level of prestraining is close to the uniform elongation of the material; above this limit specimens start to neck. The specimen shape was optimized to produce a 200mm$\times$100mm zone at the center of the specimen where strain is uniform.

C	Si	Mn	P	S	Ti	N
0.051	0.20	1.95	0.007	0.0015	0.012	0.004

Other alloying elements: Ni, Cr, Cu, Nb.

Table 1: Nominal chemical composition (weight %).

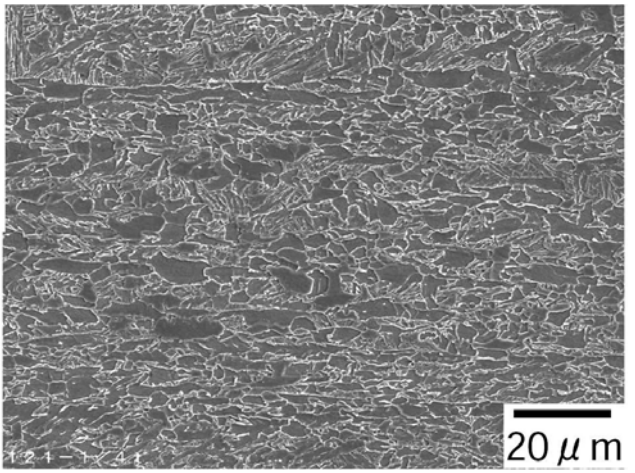

Figure 1: Plate microstructure consisting of fine polygonal ferrite and bainite (Nital etching, SEM observation).

Strain gauges were glued on the specimen to check the prestrain level. Prestrain is performed along the T direction which corresponds to the prestraining direction during UOE forming of pipes.

Mechanical testing. A comprehensive characterisation of the mechanical properties of the material was carried out along the different material directions using several specimen geometries which are displayed on Fig. 3. All tests were performed at room temperature on a servo-hydraulic testing machine. Tests were performed on both initial and prestrained materials.

Plastic behavior

Plastic anisotropy. Nominal stress–strain curves obtained for smooth bars tested along the L, D and T directions are shown on Fig. 4 for the as received material and the 6% prestrained material. The nominal strain rate is 5.10^{-4} s^{-1}. Strain is computed using the machine load line displacement

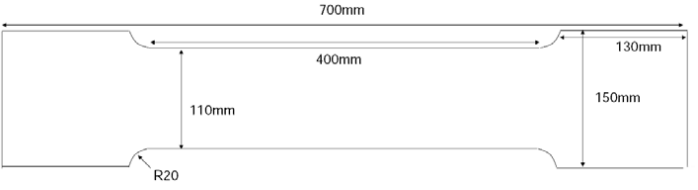

Figure 2: Large specimen used to prestrain the material.

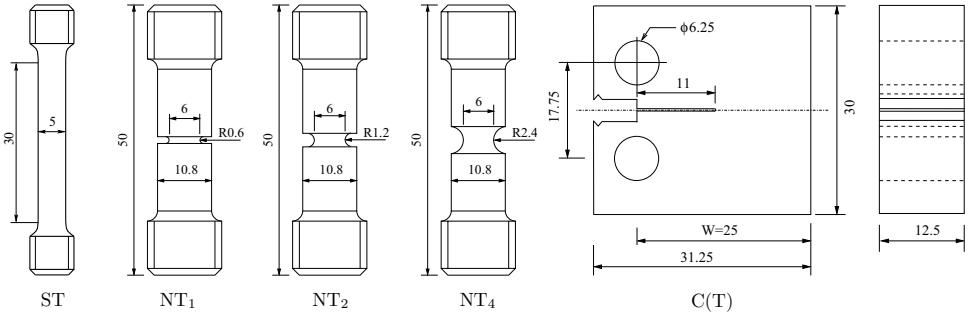

Figure 3: Samples for mechanical testing: Smooth tensile bars (ST), notched tensile bars with different notch radii (NT_1, NT_2, NT_4), C(T) specimens.

	T–0%	L–0%	D–0%	T–6%	L–6%	D–6%
YS (MPa)	567	538	500	851	621	694
UTS (MPa)	771	741	708	851	794	790
UE (%)	9.2	9.8	10.	0.	2.6	2.1
A (%)	19	21	22	12	14	14
$\mathcal{L}$	0.67	0.40	1.0	—	—	—

Table 2: Tensile properties: YS: flow stress at 0.2% plastic strain, UTS: ultimate tensile strength, UE: uniform elongation, A: macroscopic fracture strain, $\mathcal{L}$: Lankford coefficient

corrected for elastic deformation of both the load line and the specimen. This allows to compare the different curves beyond necking.

In the as received state, plastic anisotropy is evidenced: (i) flow stresses depend on the loading direction (T being the harder direction and D the softer) (ii) plastic flow is anisotropic as evidenced by the macroscopic fracture surface shown on Fig. 4-a. Lankford coefficients are obtained (before the onset of necking) by measuring diameter variation along the S direction together with axial elongation. The Lankford coefficient is defined as: $\mathcal{L} = \varepsilon_\perp/\varepsilon_S$ where ε_S is the deformation along the S direction and $\varepsilon_\perp$ the direction perpendicular to both the loading direction and the S direction. $\mathcal{L}$ is computed for strains between 3 and 7% so that it is computed only in the case of the as received material. $\mathcal{L}$ is much lower than 1 for the T and L directions and close to 1 along the D direction evidencing a strong deformation anisotropy (see Table 2).

In the prestrain state, necking occurs immediately in the T direction so that the material has no longer hardening capability along this direction. This is not the case for directions L and D which nevertheless exhibit a reduced uniform elongation. The macroscopic ductility is also reduced as evidenced on Fig. 4-b. The macroscopic failure strain is reduced by 6–7% for all directions.

Kinematic hardening. The different effect of prestraining (see above) on hardening capability of the three tested directions can be attributed to kinematic hardening (Bauschinger effect). Preliminary tension/compression cyclic tests (see Fig. 5) evidence the strong kinematic character of hardening

Ductility of smooth and notched bars

Macroscopic ductility. Force—diameter reduction for the various notched bars are shown on Fig. 6

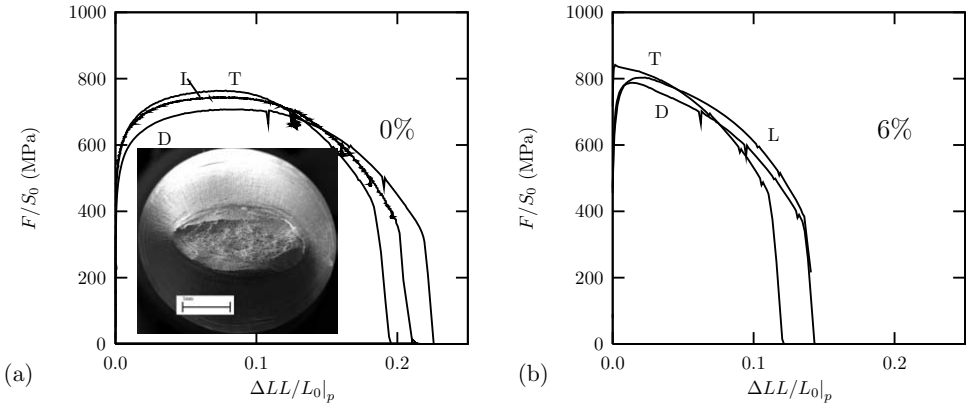

Figure 4: Tensile tests on ST bars along T, L and D directions: (a) As received material (b) 6% prestrained material. $\Delta LL/L_0|_p$: plastic elongation, F/S_0: nominal stress. (ΔLL: load line displacement, $L_0 = 30$ mm: initial gauge length F: force, S_0: initial cross section). The SEM photograph shows the macroscopic fracture surface of a specimen tested along the L direction and evidences a strong plastic anisotropy.

for the L and T directions for the as received and prestrained materials. Diameter reduction is measured along the S direction which always presents the larger variation. The following conclusions can be drawn:

- In agreement with tensile tests, maximum loads are always higher for tests carried out in the T direction compared to those in the L direction.
- Ductility, measured using the area reduction at fracture Z, decreases with notch severity as can be expected from earlier studies [2]. Z is lower in the T-direction compared to the L-direction. Z is reduced for prestrained materials (between 3 and 6%).
- In all cases, experiments present a sharp load drop which corresponds to the initiation of a macroscopic crack at the centre of the specimens. The relative diameter reduction at crack

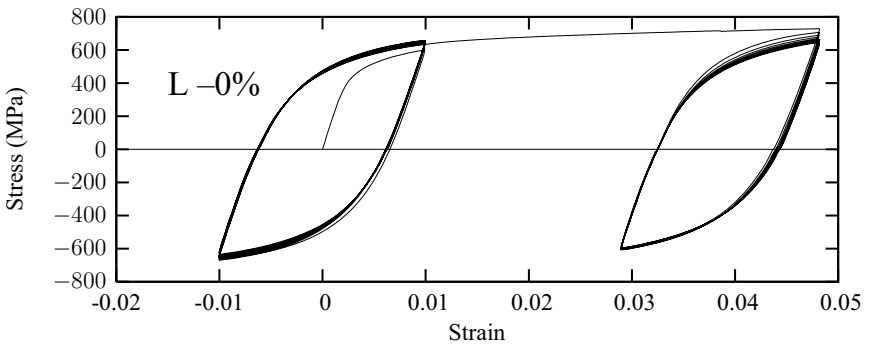

Figure 5: Tension/compression cyclic test performed in the L direction (as received material).

initiation is referred to as: $E_c = \Delta\Phi_S/\Phi_0|_c$. Values for this parameter are gathered on Fig. 7-a for the various specimen types. E_c decreases continuously with increasing notch severity for the as received material. In the case of the prestrained material, it is observed that E_c is smaller for NT_2 specimens than for NT_1 specimens (see Fig. 6 and Fig. 7). Note that in that case, the reduction at fracture is still higher for NT_2 specimens.

- In some cases, delamination is observed as shown on Fig. 6 for a NT_1 specimens in the prestrained material (dashed line).
- The material therefore presents a rupture anisotropy where the T direction is less ductile than the L direction.
- Prestrain induces a decrease the ductility on smooth and notched bars ; this decrease is of same order of magnitude than the prestrain level.

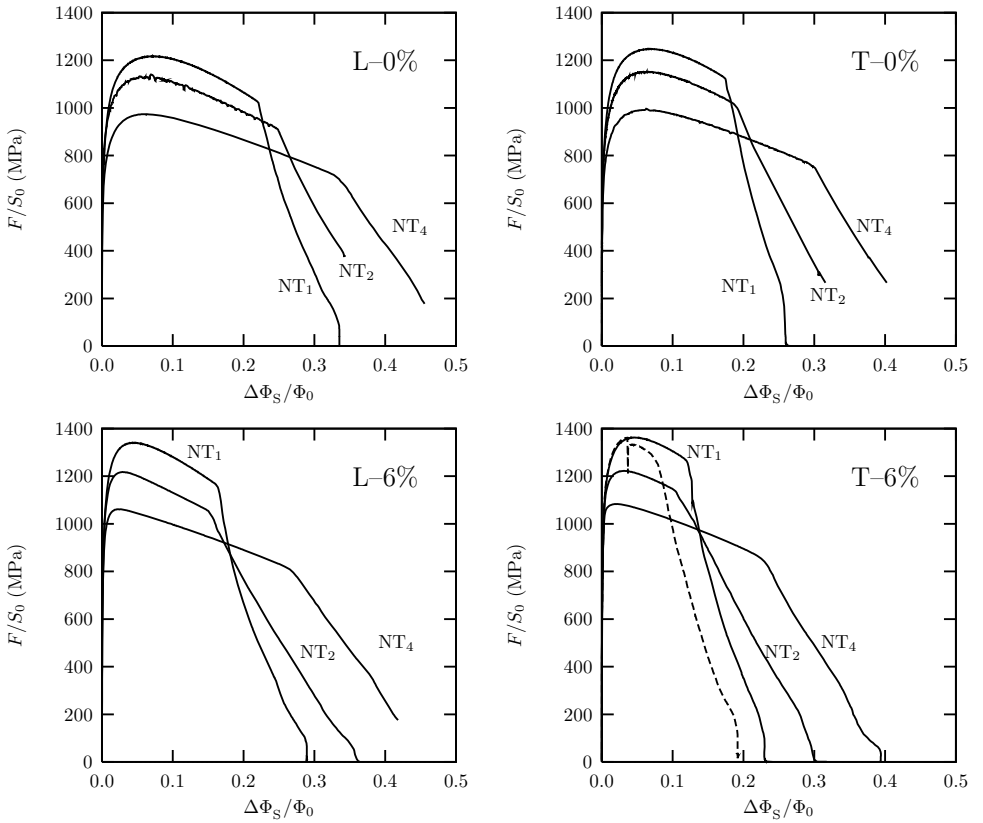

Figure 6: Force—diameter reduction curves for notched specimens tested in the T and L directions for 0% and 6% prestrain. (F: applied force, S_0: initial minimum cross section, $\Delta\Phi_S$ diameter reduction along the S direction, Φ_0: initial diameter of the minimum cross section). The dashed line (NT_1 sample, T-direction 6% prestrain corresponds to a case where delamination was observed.

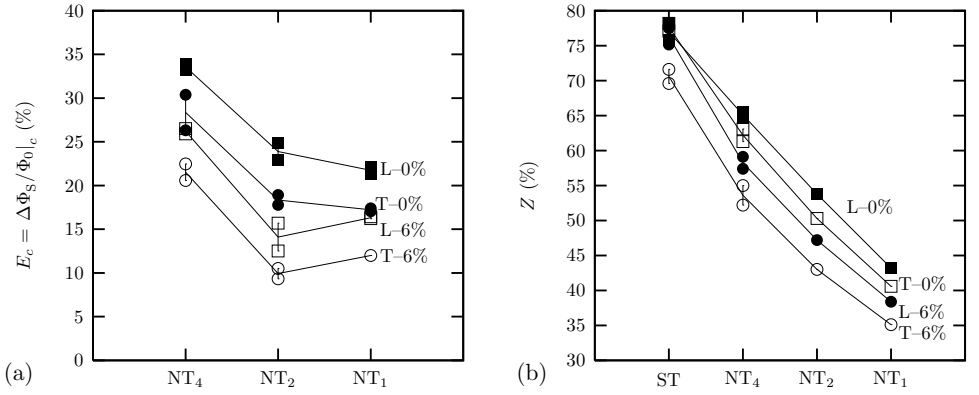

Figure 7: Effect of prestrain on ductility: (a) Diameter reduction (S-direction) at crack initiation in NT_4, NT_2 and NT_1 test specimens (T and L directions 0% and 6% prestrain). (b) Area reduction at fraction in ST, NT_4, NT_2 and NT_1 test specimens (T and L directions 0% and 6% prestrain).

Failure mechanisms. Fracture surfaces of smooth and notched tensile bars were observed using SEM. All specimens present a cup-cone fracture pattern (see e.g. Fig. 4-a). The center of the fracture surface was closely examined as it corresponds to the location of crack initiation. Results are presented for the as received material loaded in the T direction on Fig. 8. In the case of ST and NT_4 specimens, two populations of dimples can be evidenced: (i) large dimples (about 20 μm) initiated at oxides (mainly TiO_2), (ii) small dimples (about 1 μm) probably initiated at iron carbides. Large (resp. small) dimples will be referred to as primary (resp. secondary) dimples. On NT_2 and NT_1 specimens, the amount of primary dimples is increased. This indicates that particles at the origin of primary dimples nucleate first. A high level of plastic strain is needed to nucleate secondary dimples which are observed at locations where stress triaxiality is not high enough to promote rapid failure by internal necking between primary dimples. Similar conclusions are drawn from the observation of samples tested in the L direction and of samples machined in the prestrained material.

Toughness

Crack growth resistance was investigated using C(T) specimens with a total thickness $B = 12.5$ mm. Specimens without side grooves were used. C(T) specimens were fatigue-precracked in order to obtain an initial crack length a_0 about equal to $0.57W$ (see Fig. 3). The J—Δa resistance curve was determined in accordance with the ASTM-1820 standard. Ductile crack extension was determined from direct measurements of crack advance of specimens which were broken at liquid nitrogen temperature after unloading.

Results are shown on Fig. 9. Toughness anisotropy is studied by testing the L-T (i.e load is applied along the L direction and the crack advance direction corresponds to the T direction) and T-L configurations. It is observed that crack growth resistance is lower for the T-L configuration which is consistent with the lower ductilities observed on smooth and notched tensile bars tested along the T direction. Prestrain has a large effect on ductility. Values of J for a 1 mm crack advance are reduced by 28% for the L-T configuration and by 40% for the T-L configuration.

Observation of fracture surfaces, shows that the main damage mechanism is void growth of primary dimples as in severely notched tensile bars. This observation is indeed consistent with the high

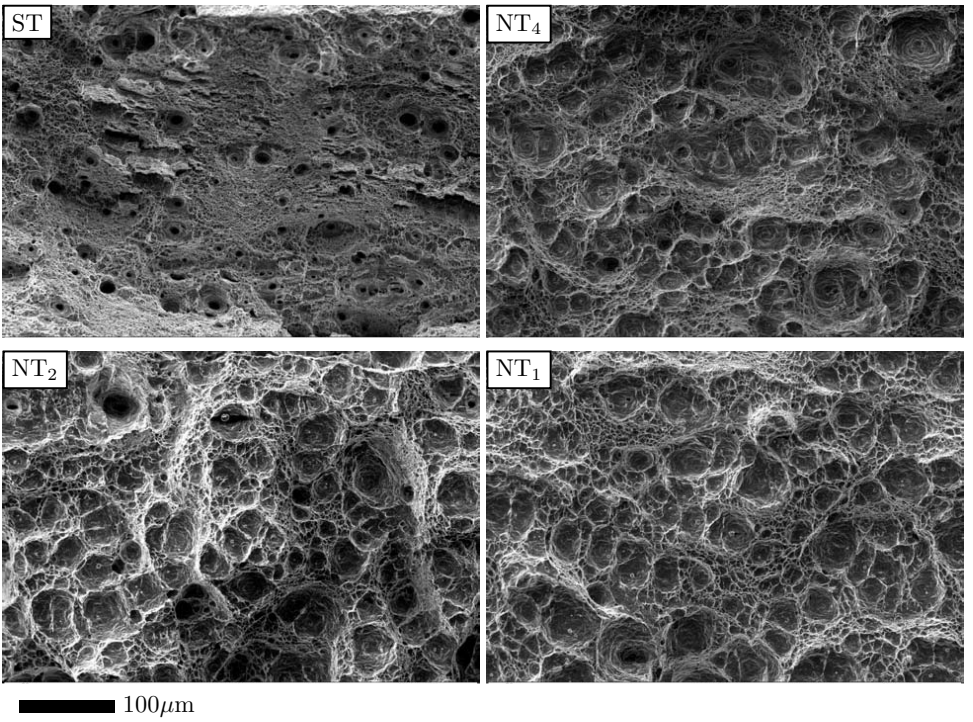

Figure 8: Fracture surfaces of ST, NT_4, NT_2 and NT_1 specimens (tested along the T direction) showing the increasing proportion of primary cavities with increasing notch severity (i.e. increasing stress triaxiality).

stress triaxiality ratio present in these specimens.

Conclusions

The mechanical and damage behavior of a X100 steel is studied in this work. Results show both a plastic and rupture anisotropy: the T direction exhibits the higher ultimate stress but the lowest ductility and toughness. A 6% prestrain in the T direction was applied to the material using large tensile specimens. Prestrain induces a slight decrease of ductility (3 to 7%) but has large effect of toughness in particular in the prestrain direction (40%).

A model able to represent the plastic and damage behaviour of the material before and after prestrain is currently under development. The model should incorporate plastic anisotropy [3], kinematic hardening [4], void growth the primary cavities [5], nucleation of secondary voids on carbides. Anisotropic plasticity and kinematic hardening should be coupled with damage development [1, 6]. Ductility and toughness anisotropy can be the result of anisotropic plasticity as different stress states may develop depending on the loading direction or of anisotropic void growth [7, 8].

References

[1] Bron, F. and Besson, J. (2006) *Engng Fract. Mech.*, 73, 1531Ű1552.

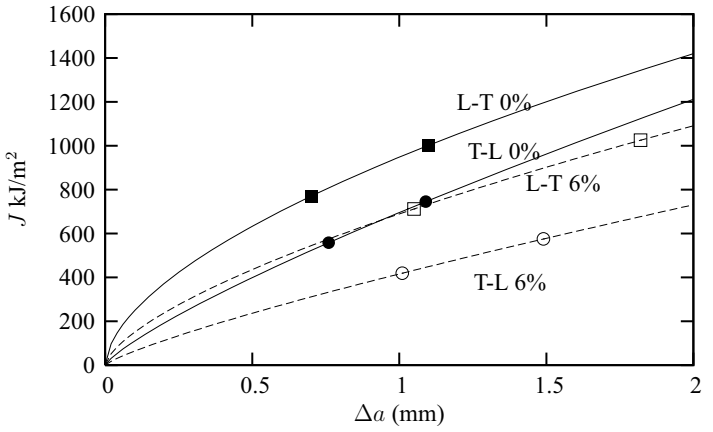

Figure 9: J—$\langle\Delta a\rangle$ curves for L-T and T-L configurations. Small (resp. large) dots correspond to specimens with (resp. without) side grooves. The average crack growth Δa is computed according to ASTM-1820 standard.

[2] Tanguy, B., Luu, T., Perrin, G., Pineau, A. and Besson, J. (2008) *Int. J. of Pressure Vessels and Piping*, (85), 322–335.

[3] Bron, F. and Besson, J. (2004) *Int. J. Plasticity*, 20, 937–963.

[4] (1990) *Mechanics of Solid Materials*. Cambridge University Press, Cambridge, U.K.

[5] Tvergaard, V. (1990) *Advances in Applied Mechanics*, 27, 83–151.

[6] Besson, J. and Guillemer-Neel, C. (2003) *Mechanics of Materials*, 35, 1–18.

[7] Pardoen, T. and Hutchinson, J. (2000) *J. Mech. Phys. Solids*, 48 (12), 2467–2512.

[8] Benzerga, A., Besson, J. and Pineau, A. (2004) *Acta Mater.*, 52, 4639–4650.